

1 **Longitudinal 7T MRI reveals volumetric changes in subregions of human medial**
2 **temporal lobe to sex hormone fluctuations**

3 Rachel G. Zsido¹, Angharad N. Williams^{1,2}, Claudia Barth^{3,4}, Bianca Serio^{1,5}, Luisa
4 Kurth¹, Frauke Beyer^{1,6}, A. Veronica Witte^{1,6}, Arno Villringer^{1,5,6}, Julia Sacher^{1,5,6}

5 ¹Max Planck Institute for Human Cognitive and Brain Sciences, Leipzig, Germany

6 ²Department of Psychology, School of Social Sciences, Nottingham Trent University,
7 Nottingham, United Kingdom

8 ³Department of Psychiatric Research, Diakonhjemmet Hospital, Oslo, Norway

9 ⁴Norwegian Centre for Mental Disorders Research, Institute of Clinical Medicine,
10 University of Oslo, Oslo, Norway

11 ⁵Max Planck School of Cognition, Leipzig, Germany

12 ⁶Clinic for Cognitive Neurology, University Medical Center Leipzig, Germany

13 The hippocampus and surrounding medial temporal lobe (MTL) are critical for memory
14 processes, with local atrophy linked to memory deficits. Animal work shows that MTL
15 subregions densely express sex hormone receptors and exhibit rapid structural
16 changes synchronized with hormone fluctuations. Such transient effects in humans
17 have thus far not been shown. By combining a dense-sampling protocol, ultra-high field
18 neuroimaging and individually-derived segmentation analysis, we demonstrate how
19 estradiol and progesterone fluctuations affect MTL subregion volumes across the
20 human menstrual cycle. Twenty-seven healthy women (19-34 years) underwent 7T
21 MRI at six timepoints to acquire T1-weighted and T2-weighted images. Linear mixed-
22 effects modeling showed positive associations between estradiol and
23 parahippocampal cortex volume, progesterone and subiculum and perirhinal Area 35
24 volumes, and an estradiol*progesterone interaction with CA1 volume. We confirmed
25 volumetric changes were not driven by hormone-related water (cerebral spinal fluid) or
26 blood-flow (pulsed arterial spin labeling) changes. These findings suggest that sex
27 hormones alter structural brain plasticity in subregions that are differentially sensitive
28 to hormones. Mapping how endogenous endocrine factors shape adult brain structure
29 has critical implications for women's health during the reproductive years as well as
30 later in life, such as increased dementia risk following perimenopause, a period of
31 pronounced sex hormone fluctuations.

32 Introduction

33 Ovarian hormones are powerful modulators of neuroplasticity, with animal
34 research offering robust evidence of endocrine regulation of brain morphology on a
35 rapid timescale (1, 2). In the timescale of hours-to-days, rodent and non-human
36 primate studies have demonstrated that estradiol and progesterone elicit modulatory
37 effects on cell proliferation (2), dendritic spine and synapse density (3-6), mitochondrial
38 and synaptic health (7, 8), and myelination (9, 10), suggesting a pivotal role of ovarian
39 hormones in brain structural organization. In humans, the menstrual cycle provides an
40 opportunity to study how endogenous fluctuations in hormones may transiently
41 influence the brain, as estradiol levels increase 8-fold and progesterone levels 80-fold
42 over a period of approximately 25-32 days (11). While a growing number of menstrual
43 cycle studies suggest that ovarian hormone fluctuations do influence brain function and
44 behavior in humans (12-15), it remains less clear how endocrine factors may shape
45 brain structure following the rhythmic nature of the menstrual cycle, and the
46 implications this would have for human adult neuroplasticity.

47 In this context, the hippocampus is a key region shown to display a remarkable
48 degree of neuroplasticity (16-18) and to be implicated in emotional regulation and
49 cognition (2, 19-21), domains that are susceptible to cycle-dependent fluctuations (22,
50 23). The hippocampus and extended medial temporal lobe (MTL) are also rich in
51 estradiol and progesterone receptors (24-26), and previous studies suggest that
52 estradiol-dominant menstrual cycle phases are associated with greater hippocampal
53 volume (27-29). Findings have been inconsistent, however, as menstrual cycle studies
54 typically only assess two timepoints and do not directly measure ovarian hormone
55 levels, rather using cycle phase as a proxy for hormone states (28, 29). In a single-
56 subject pilot study (30), we observed that subtle gray matter density changes in the
57 hippocampus paralleled daily fluctuations in endogenous estradiol levels across the
58 menstrual cycle, a dynamic pattern that would have been overlooked with a sparse
59 sampling approach. Thus, the hippocampus and surrounding MTL are promising
60 targets for cycle-related hormonal modulation of structural brain plasticity, but study
61 designs require densely-sampled hormone and neuroimaging data over the timescale
62 of the entire menstrual cycle to best capture intra- and interindividual variability in both
63 cycle variation and brain structure.

64 Moreover, while most human magnetic resonance imaging (MRI) studies treat
65 the hippocampus as a homogenous structure, recent advances in neuroimaging allow

66 for more precise delineation of neuroanatomical subregions of the hippocampus and
67 MTL *in vivo* in humans (31-34). This specificity is critical given the unique
68 cytoarchitecture, chemoarchitecture, and circuitry of MTL subregions (34-36) that
69 differentially contribute to aging and disease (37, 38). Subregion-specific architecture
70 and circuitry, alongside potential differences in hormone receptor densities (39),
71 suggest that hormone-modulated volumetric changes may manifest differently across
72 the MTL complex. Supporting evidence for the influence of ovarian hormone
73 fluctuations on subregions mainly stems from animal work, with particular emphasis
74 on the cornu ammonis 1 (CA1), a subregion critical for memory integration (40) and in
75 which neuronal loss has been associated with Alzheimer's disease (41). Estradiol
76 enhances synaptogenesis and spine density in rodent and non-human primate CA1
77 neurons, while progesterone inhibits this effect (3, 5, 42, 43). Another study in female
78 primates found that estradiol treatment increases pre- and post-synaptic proteins in
79 CA1, while combined estradiol and progesterone decreases these synaptic proteins
80 (44). Another region of key interest is perirhinal Area 35, corresponding to the
81 transentorhinal region and medial perirhinal cortex (31, 45), in which atrophy has been
82 associated with cognitive decline as well as early stages of dementia (45-49). While
83 this subregion has received little attention in regards to endogenous hormone
84 fluctuations, women have greater risk of developing Alzheimer's disease relative to
85 men, particularly following periods of more pronounced hormone fluctuations later in
86 life, such as after perimenopause (50-52). Thus, understanding how subtle hormone
87 fluctuations may influence CA1 and Area 35 volume in young women would potentially
88 provide insight into underlying mechanisms of risk for cognitive decline in women.

89 Initial evidence for hormone-modulated changes across human MTL subregions
90 has been observed in a recent single-subject study using 3T MRI, in which the authors
91 observed associations between daily ovarian hormone levels and MTL complex
92 volumes (53). No study has yet to apply a high-density sampling protocol to test
93 whether consistent patterns of hormone-volume associations at the subregion level
94 can be identified in the human hippocampus and surrounding MTL in multiple
95 participants across the menstrual cycle. To shed further light on hormone-associated
96 hippocampal and MTL changes in the female brain, we provide a densely-sampled and
97 detailed ultra-high field neuroimaging dataset in 27 healthy participants, who
98 underwent 7T MRI scanning during six menstrual cycle phases: menstrual, pre-
99 ovulatory, ovulation, post-ovulatory, mid-luteal, and premenstrual. We utilized

100 Automated Segmentation of Hippocampal Subfields software (ASHS (32)), which
101 allows for a sensitive approach to individual differences in MTL subregion morphology
102 (54). Notably, the chosen Magdeburg Young Adult 7T Atlas (31) leverages new
103 information on anatomical variability, resulting in more sophisticated delineation of the
104 boundary between the CA1 and subiculum as well as the parahippocampal cortex, and
105 further segmentation of the perirhinal region into Areas 35 and 36. We developed a
106 systematic protocol for rigorous cycle phase characterization to overcome inaccuracy
107 of menstrual cycle monitoring, a limitation of previous work in this field (55, 56). Based
108 on our pilot study (30), we hypothesized that cycle-related increases in estradiol levels
109 would be associated with increases in whole hippocampus volume. Within the
110 subregions, based on the above-mentioned animal literature, we hypothesized that
111 estradiol levels would be positively associated with perirhinal Area 35 volume, and that
112 there would be an interaction between estradiol and progesterone levels in CA1
113 volume. The other subregion volumes (CA2, CA3, subiculum, dentate gyrus, Area 36,
114 entorhinal and parahippocampal cortices) were assessed in an exploratory fashion.
115 Given the essential role of the hippocampus and MTL in adult neuroplasticity, these
116 findings may contribute to a better understanding of how endocrine factors shape
117 healthy adult brain dynamics as well as inform more individualized strategies for
118 neuroimaging the MTL complex.

119

120 **Results**

121 **Monitoring**

122 All participants were of reproductive age (mean \pm SD, 25.33 \pm 3.64 years) with a
123 healthy body mass index (BMI, 22.37 \pm 2.69 kg/m²) and regular menstrual cycle length
124 (29.04 \pm 2.62 days). Endogenous hormone values, subregion volumes, and whole
125 hippocampus volume (sum of CA1, CA2, CA3, subiculum, dentate gyrus, and
126 remaining tail) were within expected ranges (**Figure 1, Table 1**). For further analyses,
127 hormone values were log-transformed and bilateral subregion volumes were adjusted
128 for total brain volume, and statistical significance was accepted at a Benjamini-
129 Hochberg false detection rate (FDR) corrected threshold of $q < 0.05$ (see Methods for
130 additional monitoring and statistical details).

131

132

133 **Control analyses**

134 Previous work in the field has been critiqued for not taking into account potential
135 hormone-related water shifts or blood flow changes in the brain, which could be
136 misconstrued as hormone-related brain volume changes. While the Magdeburg Young
137 Adult 7T Atlas does exclude the alveus, fimbria, cerebrospinal fluid (CSF), and blood
138 vessels, we additionally assessed CSF and blood flow changes in the hippocampus
139 and did not observe statistically significant associations with estradiol (CSF: $\beta = 4.28$,
140 95% CI = -14 to 6, random effects SD = 22.62, $p = 0.402$) (blood flow: $\beta = 1.23$, 95%
141 CI = -3 to 1, random effects SD = 4.19, $p = 0.195$) nor progesterone (CSF: $\beta = 3.67$,
142 95% CI = -1 to 8, random effects SD = 22.43, $p = 0.134$) (blood flow: $\beta = 0.06$, 95% CI
143 = -1 to 1, random effects SD = 4.22, $p = 0.899$), giving further confidence that the
144 following results were not erroneously driven by these factors.

145

146 **Ovarian hormones and MTL volumes across the menstrual cycle**

147 As hypothesized, linear mixed-effects modeling showed positive associations
148 between estradiol levels and whole hippocampus volume ($\beta = 108.26$, 95% CI = 27 to
149 190, random effects SD = 174.47, $p = 0.009$). In MTL subregions, the addition of the
150 estradiol*progesterone interaction to the model significantly improved model fit only for
151 the CA1 ($\chi^2(1) = 7.691$, $p = 0.006$) (**Figure 2A**). Estradiol was positively associated
152 with CA1 volume ($\beta = 42.87$, 95% CI = 21 to 65, $p < 0.001$), progesterone was
153 negatively associated with CA1 volume ($\beta = -150.02$, 95% CI = -249 to -51, $p = 0.003$),
154 and we observed a significant interaction of estradiol and progesterone with CA1
155 volume ($\beta = 53.06$, 95% CI = 16 to 90, random effects SD = 44.03, $p = 0.005$), such
156 that at higher progesterone levels, the positive effect of estradiol on CA1 volume is
157 attenuated. Progesterone was positively associated with subiculum volume ($\beta = 13.12$,
158 95% CI = 4 to 22, random effects SD = 43.29, $p = 0.006$) (**Figure 2B**) and with Area
159 35 volume ($\beta = 11.98$, 95% CI = 2 to 21, random effects SD = 44.01, $p = 0.014$) (**Figure**
160 **2C**). Finally, estradiol was positively associated with parahippocampal cortex volume
161 ($\beta = 24.33$, 95% CI = 10 to 39, random effects SD = 32.48, $p = 0.001$) (**Figure 2D**). All
162 four subregions showed significant changes in volume over the six cycle phase
163 timepoints (**Figure 2 column 2**), but such cycle phase effects did not survive correction
164 for multiple comparisons in the whole hippocampus or subiculum. We did not observe
165 any significant relationship between hormones and CA2, CA3, dentate gyrus,
166 entorhinal cortex, or Area 36 volumes ($0.196 \leq p's \leq 0.884$).

167 **Discussion**

168 In this study, we combined dense hormone sampling with individually-derived
169 high resolution MTL segmentation analysis to demonstrate how estradiol and
170 progesterone fluctuations affect MTL and hippocampal subregion volumes.
171 Parahippocampal cortex, Area 35, subiculum, and CA1 volumes showed significant
172 changes in association with hormone fluctuations across the menstrual cycle. More
173 specifically, estradiol levels were positively associated with parahippocampal cortex
174 volume, and progesterone levels were positively associated with subiculum and Area
175 35 volume. We also observed an estradiol*progesterone level interaction with CA1
176 volume. The observed volumetric changes and their unique associations with ovarian
177 hormones, especially progesterone, were concealed when analyzing the hippocampus
178 as a whole, a potential limitation for neuroimaging studies that assess the hippocampus
179 as a single homogenous structure. Finally, we provided further confidence that the
180 observed effects do not erroneously stem from extra-neuronal factors, such as
181 hormone-induced changes in regional blood flow or CSF expansion, as we did not find
182 associations between these factors CSF and ovarian hormone levels. Taken together,
183 our results suggest that ovarian hormones rapidly alter structural brain plasticity in
184 subfields that may be differentially sensitive to hormones.

185 We were especially interested in CA1 and Area 35 given previously observed
186 selective patterns of neuronal vulnerability to memory impairment in CA1 (41) and Area
187 35 (45-49), as women are more likely to suffer from cognitive impairment when ovarian
188 hormones rapidly fluctuate, such as during perimenopause (50-52). The hypothesized
189 interaction in CA1 is in line with previous animal work, showing that estradiol enhances
190 synaptogenesis, spine density, and synaptic protein levels in CA1, while subsequent
191 increases in progesterone seem to inhibit this effect (3, 5, 8, 42-44). Moreover,
192 progesterone administration decreases dendritic spines in rodent CA1 neurons, an
193 effect that can be inhibited with a progesterone receptor antagonist (3). Although
194 studies in humans are limited and larger brain volume does not necessarily imply better
195 function, we do know that CA1 plays a distinct functional role in memory integration
196 and inference (40). Clinical studies have also shown that estrogen replacement is
197 associated with maintaining cognitive function in older age while progesterone may
198 counteract the benefit of estradiol's cognitive enhancing effect (57-63). Thus, our
199 findings are consistent with previous animal and clinical work, suggesting a

200 proliferative effect of estradiol and suppressive effect of progesterone on synaptic
201 plasticity in CA1, a region critical for cognitive processes.

202 We also observed a positive association between progesterone levels and Area
203 35 volume, which corresponds to the transentorhinal region and medial perirhinal
204 cortex (31, 45). This region is clinically relevant with regards to aging and disease, with
205 previous work showing that neurodegeneration and atrophy in this region is associated
206 with early stages of dementia and cognitive decline (45-49). Given the increasing focus
207 on the interplay between endogenous hormone fluctuations, the MTL, and the
208 disproportionate risk for Alzheimer's disease in women (51, 52), we hypothesized that
209 estradiol fluctuations would be associated with Area 35 volumetric changes. The
210 observed progesterone association is a novel finding, as the majority of related
211 literature on hippocampal structural plasticity has thus far focused on estradiol relative
212 to progesterone, and the CA1 and dentate gyrus relative to other MTL regions.
213 Additional emphasis on progesterone in future research is warranted given that levels
214 change approximately 80-fold over the menstrual cycle (11), and that both our current
215 findings and previous work (53) show a complex role of progesterone on MTL
216 subregion volumes. We note that, while the single-subject study (53) also observed
217 both positive and negative associations between progesterone and subregion
218 volumes, our observed progesterone findings occurred in different areas of the MTL,
219 where the other study observed associations with CA2/3, perirhinal, entorhinal, and
220 parahippocampal cortex volumes. These differences may be partially driven by
221 differences in study design such as number of participants, scanner strength,
222 segmentation atlas used, and differences in timepoints, and we therefore encourage
223 replication of the current findings in future studies.

224 Beyond the hypothesized regions, we also observed positive associations
225 between estradiol and parahippocampal cortex volume and progesterone and
226 subiculum volume. While the effect of menstrual cycle timepoint did not survive
227 correction for multiple comparisons in the subiculum, changes in subiculum and
228 parahippocampal cortex volumes have been observed during pregnancy (64) and after
229 surgical menopause (65), respectively, both of which are times of more extreme
230 changes in ovarian hormones. The subiculum has also been previously shown to
231 display sex-specific volumetric changes in healthy cognitive aging (37) and plays an
232 important role in mediating hippocampal-cortical interactions (66), which are critically
233 involved in cognitive function and emotional regulation, processes influenced by

234 menstrual cycle phase. While we highlight the relevant strengths of the methods used
235 in this manuscript (e.g., atlas with distinction of Area 35, better boundary of subiculum
236 and parahippocampal cortex (31)), future research is required to replicate the current
237 findings in these subregions, as our study clearly demonstrates complex interactions
238 between ovarian hormones and MTL structure as a first step in understanding
239 hormone-induced modulation of brain plasticity at the subregion level.

240 Although the nature of our MRI study cannot directly evaluate the physiological
241 processes underlying MTL morphology changes, we can speculate on potential
242 hormone-induced molecular and cellular mechanisms that may contribute to
243 mesoscopic changes in regional brain volume. Animal research lends proof that
244 ovarian hormones serve as critical components of cell survival and plasticity, where
245 possible mechanisms at the microanatomical level could include cell proliferation and
246 microglial activation (2, 67), dendritic spine and synapse density (3-6), mitochondrial
247 and synaptic health (7, 8), and myelination (9, 10), which can occur in a manner of
248 hours-to-days. These hormone-induced actions can occur through activation of
249 classical estrogen (ER α and ER β) and progesterone receptors (PR), of which the MTL
250 complex is dense with (24-26). For example, previous work has shown that ER
251 antagonists and agonists can respectively decrease and increase cell proliferation in
252 the dentate gyrus (68, 69). We note that we and others (44, 53) did not, however,
253 observe volumetric changes in this region across the menstrual cycle, suggesting that
254 the MTL changes we observe may be more driven by synaptic plasticity and
255 remodeling in regions such as the CA1 as opposed to neurogenesis in the dentate
256 gyrus. Indeed, within the hippocampal complex, these three classical receptors appear
257 most prominent in the CA1 (39), where estradiol administration and ER agonists
258 increase synaptic proteins (44, 70), ER antagonists decrease synaptic proteins (71),
259 and progesterone administration and PR antagonists respectively decrease and
260 increase dendritic spines (3, 5). These modulatory effects were not as prominent in the
261 dentate gyrus and other subregions as compared to in CA1 (39, 44, 70, 71). Our study
262 thus encourages future investigation of specific biological microstructural mechanisms
263 underlying observed short-term dynamics of human MTL subregion morphology during
264 times of ovarian hormone fluctuations.

265 While the rigorous cycle monitoring protocol and individually-derived MTL
266 segmentation analyses serve as strengths of this sufficiently powered longitudinal
267 study, several limitations should be acknowledged. We recruited a healthy population

268 to reflect how endogenous endocrine factors regulate healthy adult brain structural
269 plasticity in the female reproductive years. Therefore, future studies should test
270 whether these hormone-induced changes in MTL subregions are further exacerbated
271 during times of more profound neuroendocrine change, and whether there are
272 behavioral consequences for patient populations. Recent work does suggest that early
273 changes in neuropsychiatric and neurodegenerative disease are better detected in
274 smaller subregions of the MTL rather than with whole structure analysis (46-48, 72),
275 and women are at increased risk for such disorders following ovarian hormone
276 fluctuations, such as depressive disorders (73-77), multiple sclerosis (78-80), dementia
277 (50, 52), and other inflammation-related disorders (81) during the premenstrual phase
278 (73-75, 78, 81), postpartum period (73, 76, 79), and following perimenopause (50, 52,
279 73, 77, 80). Given the essential role of the MTL in adult synaptic plasticity and the
280 differential contributions of MTL subregions to cognitive functions (40, 82-86), this
281 information may be particularly relevant for plasticity-related disorders such as
282 depression and dementia. Furthermore, while our analyses focused on the
283 hippocampal and MTL complex, ovarian hormones have widespread effects on many
284 brain areas that work in tandem. Subregions have distinct connectivity profiles (35) and
285 future studies should extend the focus to other brain areas to capture a broader
286 network understanding. Given that we saw unique hormone interactions with CA1 and
287 subiculum, and that hippocampal projections to the medial prefrontal cortex (PFC)
288 originate primarily in the CA1 and subiculum (87), we suggest investigation of
289 hormone-modulated changes in structural and functional connectivity between these
290 subregions and the PFC. The PFC also densely expresses hormone receptors (88)
291 and displays hormone-induced structural plasticity (4, 7, 8), with the hippocampal-
292 prefrontal pathway implicated in cognitive and emotional processes (66, 87).

293 Despite decades of scientific evidence for dynamic interactions between the
294 endocrine and nervous systems, neuroscientific research has largely ignored how
295 endogenous ovarian hormone fluctuations influence human adult brain structural
296 plasticity. This, alongside the current underrepresentation of female samples in
297 neuroscience (55, 89-91), directly limits opportunities for basic scientific discovery and
298 the diversity of human brain health. The MTL region has a remarkable degree of
299 plasticity in response to subtle hormone changes across the female lifespan, and our
300 findings suggest that these changes are detectable at the subregion level. To our
301 knowledge, this is the first study to use ultra-high field neuroimaging to demonstrate

302 how endogenous hormone fluctuations rapidly and transiently alter volume across the
303 MTL complex in multiple participants. We demonstrate the feasibility of such a
304 longitudinal MRI design for creating dynamic and personalized maps of the human
305 brain to inform more individualized strategies for neuroimaging the MTL, which may
306 ultimately lead to better understanding of the manifestation and treatment of hormone-
307 related neuropsychiatric and neurodegenerative diseases.

308

309 **Methods**

310 **Participants**

311 Eligible individuals were female, right-handed, 18–35 years old, with a BMI 18.5–29
312 kg/m², and without any neurological or psychiatric illness as confirmed with a
313 structured clinical interview. Exclusion criteria were prescription medication or
314 supplement use, tobacco use, positive drug or pregnancy tests, use of hormonal
315 contraceptives, or having been pregnant, postpartum, breastfeeding, or had an
316 abortion within one year of the study. Participants were screened and excluded for
317 DSM-IV Axis I Disorders (92) and Axis II Disorders (93), as well as for presence of
318 premenstrual mood symptoms using the Premenstrual Symptoms Screening Tool
319 (PSST) (94). All participants provided written informed consent after all procedures
320 were fully explained. Forty-one participants were enrolled, of whom two were excluded
321 due to inability to tolerate the 7T MRI scan, eight voluntarily discontinued due to time
322 demands of study, and four were excluded due to irregular cycles, irregularities in
323 bloodwork, or emergency contraceptive pill use after enrollment (included participants
324 N = 27). Of the included participants, twenty completed all six timepoints, two
325 completed five timepoints, one completed three timepoints, one completed two
326 timepoints, and three completed one timepoint (dropout reasons: five due to
327 scheduling conflicts, one used the emergency contraceptive pill, one got an MRI-
328 incompatible retainer); for a total of 138 assessments. The Ethical Committee at the
329 Medical Faculty of Leipzig University approved the study, protocol, and informed
330 consent forms (#077-11-07032011), and the study has been pre-registered at the
331 Open Science Framework (<https://osf.io/8mk74/>).

332

333 **Assessment timing**

334 Participants had a documented history of regular menstrual cycles. The study
335 assessments occurred during six cycle phases: menstrual (<5 days menses onset),

336 pre-ovulatory (≤ 2 days before ovulation), ovulation (≤ 24 hours of ovulation), post-
337 ovulatory (≤ 2 days after ovulation), mid-luteal (6-8 days after ovulation), and
338 premenstrual (≤ 3 next menses onset). We developed a systematic protocol for rigorous
339 menstrual cycle monitoring and characterization to determine cycle phase timing as
340 follows. After enrollment, participants used an online application
341 (<https://www.mynfp.de>) to record daily vaginal basal body temperature, menses
342 information, and cycle day and length information. To determine ovulatory timing,
343 participants underwent multiple vaginal ultrasounds to track growing follicle and detect
344 ovulation, completed luteinizing hormone urine tests throughout the ovulatory week,
345 and consulted with a gynecologist. The first assessment phase was randomized across
346 participants, and all other assessments took place in remaining chronological order
347 (menstrual, pre-ovulatory, ovulation, post-ovulatory, mid-luteal, premenstrual).

348

349 **Blood Measurements**

350 Serum from fasting-blood samples was collected at every ultrasound and
351 assessment day visit to measure hormones, confirm cycle phase, ensure physical
352 health, and exclude pregnancy or recent drug-intake. Serum was delivered
353 immediately to the hospital laboratory and kept at 5°C until assayed within 24 hours.
354 Estradiol and progesterone concentrations were determined using high performance
355 liquid chromatography-tandem mass spectrometry (LC-MS/MS), and follicle-
356 stimulating hormone and luteinizing hormone concentrations were determined using
357 electrochemiluminescence immunoassay (ECLIA; Roche). Of the 138 assessments,
358 estradiol values for two assessments and progesterone values for one assessment
359 were not included due to pre-analytical error.

360

361 **7T MRI acquisition**

362 Anatomical MRI scans were acquired at the Max Planck Institute for Human
363 Cognitive and Brain Sciences, Leipzig, using a Siemens Magnetom 7T system
364 (Siemens Healthineers, Erlangen, Germany) and 32-channel head array coil (NOVA
365 Medical Inc., Wilmington MA, USA), matched for time of day and without caffeine
366 intake. We acquired high-resolution whole-brain T1-weighted images using an
367 MP2RAGE protocol (repetition time (TR) = 5000 ms; inversion time (TI)
368 $1/2 = 900/2750$ ms; echo time (TE) = 2.45 ms; image matrix: $320 \times 320 \times 240$; voxel
369 size $0.7 \text{ mm} \times 0.7 \text{ mm} \times 0.7 \text{ mm}$; flip angle $1/2 = 5^\circ/3^\circ$; parallel imaging using GRAPPA

370 with acceleration factor = 2). We acquired T2-weighted imaging slabs perpendicular to
371 the anterior-posterior axis of the hippocampus using a Turbo-Spin Echo Sequence
372 (TR = 16000 ms; TE = 14 ms; image matrix: 384 × 384; 50 slices; voxel size:
373 0.5 mm × 0.5 mm × 1 mm; refocusing flip angle = 120°; turbo factor = 8; parallel imaging
374 using GRAPPA with acceleration factor = 2).

375

376 **MTL segmentation and volumetry**

377 Background noise removal from uniform T1-weighted MP2RAGE image
378 volumes were done using [https://github.com/JosePMarques/MP2RAGE-related-](https://github.com/JosePMarques/MP2RAGE-related-scripts)
379 [scripts](https://github.com/JosePMarques/MP2RAGE-related-scripts) (95). The high resolution T1- and T2-weighted images were then submitted to
380 the Automatic Segmentation of Hippocampal Subfields (ASHS) package (32) using the
381 Magdeburg Young Adult 7T Atlas (31), which has been shown to be more sensitive to
382 individual differences in MTL subregion morphology compared to FreeSurfer (54).
383 ASHS segmentation software uses a fully automated framework at all stages (MRI pre-
384 processing, rigid body transformation alignment of T1- and T2-weighted images, bias
385 correction and refining, etc.), automatically segmenting the MTL in the T2-weighted
386 MRI scans. ASHS documentation, atlases, and software are available
387 at <https://sites.google.com/view/ashs-dox/> and <https://www.nitrc.org/projects/ashs>,
388 with technical details and reliability described further in (32). We performed
389 segmentation and bilateral volume calculations for hippocampal (CA1; CA2; CA3;
390 subiculum; dentate gyrus) and adjacent MTL subregions (entorhinal cortex;
391 parahippocampal cortex; perirhinal cortex [segmented into Area 35 and Area 36]). ITK-
392 SNAP (v3.8) was used for quality assurance (e.g., proper alignment of T1- and T2-
393 weighted images). Quality assurance images were visually assessed by two raters
394 blinded to cycle phase. All code is publicly available at
395 <https://github.com/RGZsido/MTLPlasticity2022>.

396

397 **Total brain volume, CSF, and cerebral blood flow**

398 Total brain volume as well as CSF were calculated using the 7T T1-weighted
399 images and the Segment Data module in CAT12 toolbox of SPM12 MATLAB R2021a,
400 with all overall weighted image quality (IQR) measures > 90%. Cerebral blood flow was
401 calculated using a T1-weighted MPRAGE (TR = 2300 ms, TI = 900 ms, TE = 4.21 ms,
402 flip angle = 9°, FOV = 256 × 256 mm, slices = 176, bandwidth = 240 Hz/px, voxel
403 size = 1 × 1 × 1 mm³) and a pulsed arterial spin labeling (pASL) sequence (TR = 3000,

404 TI1 = 700 ms, T1S = 1775, TI2 = 1800ms, TE = 13 ms, flip angle = 90°, matrix size =
405 64 × 64, slices = 24, FOV = 192 × 192 mm, voxel size = 3 × 3 × 4 mm³; labeling slab
406 thickness = 100 mm with a gap of 22 mm, 101 pairs of label and control images) (96),
407 acquired on the same assessment days on a 3T Magnetom Verio scanner (Siemens,
408 Erlangen, Germany) using a 32-channel head coil. The pASL data was preprocessed
409 using an inhouse MATLAB analysis pipeline, which included co-registration to the
410 MPRAGE image, motion correction with linear regression, normalization to MNI space,
411 and smoothing with a 2D spatial Gaussian filter of 3-mm FWHM. The final cerebral
412 blood flow values used for the analysis were calculated by pairwise subtraction of
413 labeled and control images by the perfusion model (97).

414 For the cerebral blood flow analysis, an anatomical region-of-interest (ROI) was
415 created as binary mask of the hippocampus using the WFU PickAtlas toolbox. The
416 mask was resampled to a 3x3x4-mm voxel size to match the pASL images using the
417 `coregister:reslice` function in SPM12. The preprocessed cerebral blood flow maps were
418 multiplied with the binary mask of the hippocampus and the average cerebral blood
419 flow value (over all voxels within the ROI) was extracted. This was done for all
420 timepoints for each participant.

421
422 **Statistical analysis**

423 Assuming a medium effect size ($\eta^2 = 0.06$), alpha coefficient of 0.05 and a
424 power of 80 percent, we calculated a total sample size of $N = 18$ (*a priori* power
425 analysis, G*Power). In the project protocol, we stated that we aimed to include $N = 20$
426 healthy participants with all six timepoints. Estradiol and progesterone values were log-
427 transformed prior to analyses. For outlier detection in brain volumes, we flagged
428 bilateral volumes that were three standard deviations from the mean for anatomical
429 inspection by two raters. If upon inspection the volume segmentation maps were
430 unanimously deemed anatomically sound, the volumes were kept to capture
431 reasonable anatomical variation. Of the 138 assessments, we flagged a total of four
432 brain volumes, of which two were determined to be of poor segmentation quality (both
433 for CA1), and were thus removed from further analyses. Bilateral subregion volumes
434 were then adjusted for total brain volume (unstandardized residuals).

435 For control analyses, we performed linear mixed-effects modeling using the
436 maximum likelihood method of the 'lmer' function in the 'lme4' R package (v3.5.2 (98))
437 to assess potential effects of hormones (estradiol and progesterone) on CSF and

438 cerebral blood flow. For main analyses, we used linear mixed-effects models to assess
439 fixed effects of hormones as well as their interaction on whole hippocampus and on
440 each subregion volume. Inclusion of the interaction term was assessed by comparing
441 model fits using the ‘anova’ function. The p-values of the model parameters were
442 calculated via Wald tests and corrected for multiple comparisons using Benjamini–
443 Hochberg procedure (99) controlling for FDR, and were accepted at an FDR-corrected
444 threshold of $q < 0.05$. For brain volumes that showed significant effects of hormones,
445 we then investigated the fixed effects of cycle phase timepoint modelled as an
446 independent regressor, and performed post-hoc tests using the ‘diffsmeans’ function
447 and the Satterthwaite correction for degrees of freedom. Participants were included as
448 a random factor in all models. The R code for analyses is publicly available at
449 <https://github.com/RGZsido/MTLPlasticity2022>.

450

451 **Acknowledgements**

452 Preparation of this manuscript was supported by a Fellowship from the Joachim
453 Herz Foundation (RGZ), the Branco Weiss Fellowship, Society in Science, National
454 Association for Research on Schizophrenia and Depression (NARSAD) Young
455 Investigator Grant 25032 from the Brain & Behavior Research Foundation (JS), and a
456 Minerva Research Group Grant from the Max Planck Society (JS). The funders of the
457 study had no role in study design, data collection, data interpretation, or writing of the
458 report. The corresponding author had full access to all the data and final responsibility
459 for the decision to submit for publication. We thank Matthias Heinrich for assistance in
460 data acquisition, Toralf Mildner for assistance in pASL preprocessing, and Cornelia
461 Ketscher and Heike Schmidt Duderstedt for assistance with data visualization.

462

463 **Competing Interests**

464 All authors declare that no competing interests exist.

465 References

- 466
- 467 1. Been LE, Sheppard PA, Galea LA, Glasper ER (2021): Hormones and neuroplasticity: A
468 lifetime of adaptive responses. *Neuroscience & Biobehavioral Reviews*.
- 469 2. Barha CK, Galea LA (2010): Influence of different estrogens on neuroplasticity and
470 cognition in the hippocampus. *Biochimica et Biophysica Acta (BBA)-General Subjects*.
471 1800:1056-1067.
- 472 3. Woolley CS, McEwen BS (1993): Roles of estradiol and progesterone in regulation of
473 hippocampal dendritic spine density during the estrous cycle in the rat. *J Comp Neurol*.
474 336:293-306.
- 475 4. Hao J, Rapp PR, Leffler AE, Leffler SR, Janssen WG, Lou W, et al. (2006): Estrogen alters
476 spine number and morphology in prefrontal cortex of aged female rhesus monkeys. *J Neurosci*.
477 26:2571-2578.
- 478 5. Woolley CS, McEwen BS (1992): Estradiol mediates fluctuation in hippocampal synapse
479 density during the estrous cycle in the adult rat [published erratum appears in *J Neurosci* 1992
480 Oct; 12 (10): following table of contents]. *J Neurosci*. 12:2549-2554.
- 481 6. MacLusky NJ, Luine VN, Hajszan T, Leranth C (2005): The 17 α and 17 β isomers of
482 estradiol both induce rapid spine synapse formation in the CA1 hippocampal subfield of
483 ovariectomized female rats. *Endocrinology*. 146:287-293.
- 484 7. Hara Y, Yuk F, Puri R, Janssen WG, Rapp PR, Morrison JH (2014): Presynaptic
485 mitochondrial morphology in monkey prefrontal cortex correlates with working memory and
486 is improved with estrogen treatment. *Proceedings of the National Academy of Sciences*.
487 111:486-491.
- 488 8. Hara Y, Waters EM, McEwen BS, Morrison JH (2015): Estrogen effects on cognitive and
489 synaptic health over the lifecourse. *Physiol Rev*. 95:785-807.
- 490 9. Patel R, Moore S, Crawford DK, Hannsun G, Sasidhar MV, Tan K, et al. (2013):
491 Attenuation of corpus callosum axon myelination and remyelination in the absence of
492 circulating sex hormones. *Brain Pathol*. 23:462-475.
- 493 10. Arevalo M-A, Santos-Galindo M, Bellini M-J, Azcoitia I, Garcia-Segura LM (2010):
494 Actions of estrogens on glial cells: implications for neuroprotection. *Biochimica et Biophysica*
495 *Acta (BBA)-General Subjects*. 1800:1106-1112.
- 496 11. Stricker R, Eberhart R, Chevailler M-C, Quinn FA, Bischof P, Stricker R (2006):
497 Establishment of detailed reference values for luteinizing hormone, follicle stimulating
498 hormone, estradiol, and progesterone during different phases of the menstrual cycle on the
499 Abbott ARCHITECT[®] analyzer. *Clinical Chemistry and Laboratory Medicine (CCLM)*. 44:883-887.
- 500 12. Pritschet L, Santander T, Taylor CM, Layher E, Yu S, Miller MB, et al. (2020): Functional
501 reorganization of brain networks across the human menstrual cycle. *Neuroimage*.
502 220:117091.
- 503 13. Weis S, Hodgetts S, Hausmann M (2019): Sex differences and menstrual cycle effects
504 in cognitive and sensory resting state networks. *Brain Cogn*. 131:66-73.
- 505 14. Arélin K, Mueller K, Barth C, Rekkas PV, Kratzsch J, Burmann I, et al. (2015):
506 Progesterone mediates brain functional connectivity changes during the menstrual cycle—a
507 pilot resting state MRI study. *Frontiers in neuroscience*. 9:44.
- 508 15. Petersen N, Kilpatrick LA, Goharзад A, Cahill L (2014): Oral contraceptive pill use and
509 menstrual cycle phase are associated with altered resting state functional connectivity.
510 *Neuroimage*. 90:24-32.
- 511 16. Schmidt-Hieber C, Jonas P, Bischofberger J (2004): Enhanced synaptic plasticity in
512 newly generated granule cells of the adult hippocampus. *Nature*. 429:184-187.

- 513 17. Bartsch T, Wulff P (2015): The hippocampus in aging and disease: From plasticity to
514 vulnerability. *Neuroscience*. 309:1-16.
- 515 18. Sheppard PA, Choleris E, Galea LA (2019): Structural plasticity of the hippocampus in
516 response to estrogens in female rodents. *Molecular brain*. 12:1-17.
- 517 19. Frick KM, Kim J (2018): Mechanisms underlying the rapid effects of estradiol and
518 progesterone on hippocampal memory consolidation in female rodents. *Horm Behav*.
519 104:100-110.
- 520 20. Squire LR (1992): Memory and the hippocampus: a synthesis from findings with rats,
521 monkeys, and humans. *Psychol Rev*. 99:195.
- 522 21. Schumacher A, Villaruel FR, Ussling A, Riaz S, Lee AC, Ito R (2018): Ventral hippocampal
523 CA1 and CA3 differentially mediate learned approach-avoidance conflict processing. *Curr Biol*.
524 28:1318-1324. e1314.
- 525 22. Farage MA, Osborn TW, MacLean AB (2008): Cognitive, sensory, and emotional
526 changes associated with the menstrual cycle: a review. *Arch Gynecol Obstet*. 278:299-307.
- 527 23. Sundström Poromaa I, Gingnell M (2014): Menstrual cycle influence on cognitive
528 function and emotion processing—from a reproductive perspective. *Frontiers in neuroscience*.
529 8:380.
- 530 24. González M, Cabrera-Socorro A, Pérez-García CG, Fraser JD, López FJ, Alonso R, et al.
531 (2007): Distribution patterns of estrogen receptor α and β in the human cortex and
532 hippocampus during development and adulthood. *J Comp Neurol*. 503:790-802.
- 533 25. Brinton RD, Thompson RF, Foy MR, Baudry M, Wang J, Finch CE, et al. (2008):
534 Progesterone receptors: form and function in brain. *Front Neuroendocrinol*. 29:313-339.
- 535 26. Österlund MK, Grandien K, Keller E, Hurd YL (2000): The human brain has distinct
536 regional expression patterns of estrogen receptor α mRNA isoforms derived from alternative
537 promoters. *J Neurochem*. 75:1390-1397.
- 538 27. Lisofsky N, Mårtensson J, Eckert A, Lindenberger U, Gallinat J, Kühn S (2015):
539 Hippocampal volume and functional connectivity changes during the female menstrual cycle.
540 *Neuroimage*. 118:154-162.
- 541 28. Protopopescu X, Butler T, Pan H, Root J, Altemus M, Polanecsky M, et al. (2008):
542 Hippocampal structural changes across the menstrual cycle. *Hippocampus*. 18:985-988.
- 543 29. Pletzer B, Kronbichler M, Aichhorn M, Bergmann J, Ladurner G, Kerschbaum HH (2010):
544 Menstrual cycle and hormonal contraceptive use modulate human brain structure. *Brain Res*.
545 1348:55-62.
- 546 30. Barth C, Steele CJ, Mueller K, Rekkas VP, Arélin K, Pampel A, et al. (2016): In-vivo
547 dynamics of the human hippocampus across the menstrual cycle. *Scientific reports*. 6:1-9.
- 548 31. Berron D, Vieweg P, Hochkeppeler A, Pluta J, Ding S-L, Maass A, et al. (2017): A protocol
549 for manual segmentation of medial temporal lobe subregions in 7 Tesla MRI. *NeuroImage*:
550 *Clinical*. 15:466-482.
- 551 32. Yushkevich PA, Pluta JB, Wang H, Xie L, Ding SL, Gertje EC, et al. (2015): Automated
552 volumetry and regional thickness analysis of hippocampal subfields and medial temporal
553 cortical structures in mild cognitive impairment. *Hum Brain Mapp*. 36:258-287.
- 554 33. Ding SL, Royall JJ, Sunkin SM, Ng L, Facer BA, Lesnar P, et al. (2016): Comprehensive
555 cellular-resolution atlas of the adult human brain. *J Comp Neurol*. 524:3127-3481.
- 556 34. Ding SL, Van Hoesen GW (2015): Organization and detailed parcellation of human
557 hippocampal head and body regions based on a combined analysis of cyto-and
558 chemoarchitecture. *J Comp Neurol*. 523:2233-2253.
- 559 35. Duvernoy HM, Cattin F, Risold P-Y (2005): *The human hippocampus: functional*
560 *anatomy, vascularization and serial sections with MRI*. Springer.

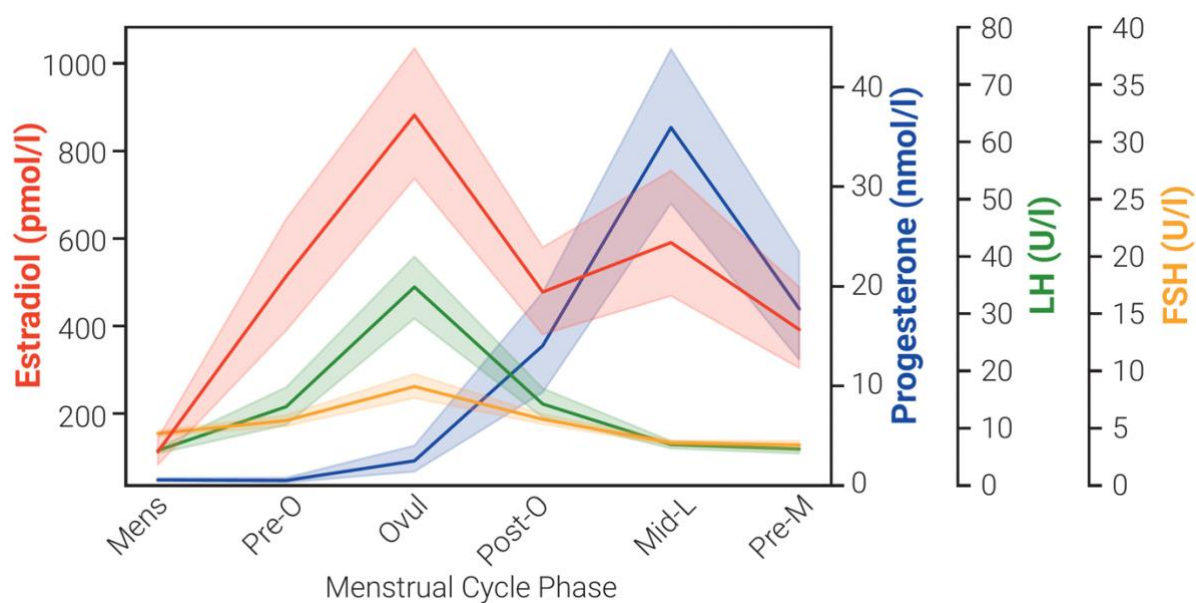
- 561 36. Amunts K, Kedo O, Kindler M, Pieperhoff P, Mohlberg H, Shah N, et al. (2005):
562 Cytoarchitectonic mapping of the human amygdala, hippocampal region and entorhinal
563 cortex: intersubject variability and probability maps. *Anat Embryol (Berl)*. 210:343-352.
- 564 37. Malykhin NV, Huang Y, Hrybouski S, Olsen F (2017): Differential vulnerability of
565 hippocampal subfields and anteroposterior hippocampal subregions in healthy cognitive
566 aging. *Neurobiol Aging*. 59:121-134.
- 567 38. de Flores R, La Joie R, Landeau B, Perrotin A, Mézenge F, de La Sayette V, et al. (2015):
568 Effects of age and Alzheimer's disease on hippocampal subfields: comparison between manual
569 and FreeSurfer volumetry. *Hum Brain Mapp*. 36:463-474.
- 570 39. Mitterling KL, Spencer JL, Dziedzic N, Shenoy S, McCarthy K, Waters EM, et al. (2010):
571 Cellular and subcellular localization of estrogen and progesterin receptor immunoreactivities in
572 the mouse hippocampus. *J Comp Neurol*. 518:2729-2743.
- 573 40. Schlichting ML, Zeithamova D, Preston AR (2014): CA1 subfield contributions to
574 memory integration and inference. *Hippocampus*. 24:1248-1260.
- 575 41. West MJ, Coleman PD, Flood DG, Troncoso JC (1994): Differences in the pattern of
576 hippocampal neuronal loss in normal ageing and Alzheimer's disease. *The Lancet*. 344:769-
577 772.
- 578 42. Hao J, Janssen WG, Tang Y, Roberts JA, McKay H, Lasley B, et al. (2003): Estrogen
579 increases the number of spinophilin-immunoreactive spines in the hippocampus of young and
580 aged female rhesus monkeys. *J Comp Neurol*. 465:540-550.
- 581 43. Bali N, Arimoto JM, Iwata N, Lin SW, Zhao L, Brinton RD, et al. (2012): Differential
582 responses of progesterone receptor membrane component-1 (Pgrmc1) and the classical
583 progesterone receptor (Pgr) to 17 β -estradiol and progesterone in hippocampal subregions
584 that support synaptic remodeling and neurogenesis. *Endocrinology*. 153:759-769.
- 585 44. Choi JM, Romeo RD, Brake WG, Bethea CL, Rosenwaks Z, McEwen BS (2003): Estradiol
586 increases pre- and post-synaptic proteins in the CA1 region of the hippocampus in female
587 rhesus macaques (*Macaca mulatta*). *Endocrinology*. 144:4734-4738.
- 588 45. Braak H, Braak E (1991): Neuropathological staging of Alzheimer-related changes.
589 *Acta Neuropathol (Berl)*. 82:239-259.
- 590 46. Olsen RK, Yeung L-K, Noly-Gandon A, D'Angelo MC, Kacollja A, Smith VM, et al. (2017):
591 Human anterolateral entorhinal cortex volumes are associated with cognitive decline in aging
592 prior to clinical diagnosis. *Neurobiol Aging*. 57:195-205.
- 593 47. Berron D, Vogel JW, Insel PS, Pereira JB, Xie L, Wisse LE, et al. (2021): Early stages of
594 tau pathology and its associations with functional connectivity, atrophy and memory. *Brain*.
595 144:2771-2783.
- 596 48. Krumm S, Kivisaari SL, Probst A, Monsch AU, Reinhardt J, Ulmer S, et al. (2016): Cortical
597 thinning of parahippocampal subregions in very early Alzheimer's disease. *Neurobiol Aging*.
598 38:188-196.
- 599 49. Ding SL, Van Hoesen GW, Cassell MD, Poremba A (2009): Parcellation of human
600 temporal polar cortex: a combined analysis of multiple cytoarchitectonic, chemoarchitectonic,
601 and pathological markers. *J Comp Neurol*. 514:595-623.
- 602 50. Brinton RD, Yao J, Yin F, Mack WJ, Cadenas E (2015): Perimenopause as a neurological
603 transition state. *Nature reviews endocrinology*. 11:393-405.
- 604 51. Georgakis MK, Beskou-Kontou T, Theodoridis I, Skalkidou A, Petridou ET (2019):
605 Surgical menopause in association with cognitive function and risk of dementia: a systematic
606 review and meta-analysis. *Psychoneuroendocrinology*. 106:9-19.

- 607 52. Lee BH, Puri TA, Galea LA (2021): Sex and sex hormone differences in hippocampal
608 neurogenesis and their relevance to Alzheimer's disease. *Sex and Gender Differences in*
609 *Alzheimer's Disease*: Elsevier, pp 23-77.
- 610 53. Taylor CM, Pritschet L, Olsen RK, Layher E, Santander T, Grafton ST, et al. (2020):
611 Progesterone shapes medial temporal lobe volume across the human menstrual cycle.
612 *Neuroimage*. 220:117125.
- 613 54. Sone D, Sato N, Maikusa N, Ota M, Sumida K, Yokoyama K, et al. (2016): Automated
614 subfield volumetric analysis of hippocampus in temporal lobe epilepsy using high-resolution
615 T2-weighted MR imaging. *NeuroImage: Clinical*. 12:57-64.
- 616 55. Taylor CM, Pritschet L, Jacobs EG (2021): The scientific body of knowledge—Whose
617 body does it serve? A spotlight on oral contraceptives and women's health factors in
618 neuroimaging. *Front Neuroendocrinol*. 60:100874.
- 619 56. Schmalenberger KM, Tauseef HA, Barone JC, Owens SA, Lieberman L, Jarczok MN, et
620 al. (2021): How to study the menstrual cycle: Practical tools and recommendations.
621 *Psychoneuroendocrinology*. 123:104895.
- 622 57. Rice MM, Graves AB, McCurry SM, Gibbons LE, Bowen JD, McCormick WC, et al. (2000):
623 Postmenopausal estrogen and estrogen-progestin use and 2-year rate of cognitive change in
624 a cohort of older Japanese American women: The Kame Project. *Arch Intern Med*. 160:1641-
625 1649.
- 626 58. Rapp SR, Espeland MA, Shumaker SA, Henderson VW, Brunner RL, Manson JE, et al.
627 (2003): Effect of estrogen plus progestin on global cognitive function in postmenopausal
628 women: the Women's Health Initiative Memory Study: a randomized controlled trial. *JAMA*.
629 289:2663-2672.
- 630 59. Jacobs DM, Tang M-X, Stern Y, Sano M, Marder K, Bell K, et al. (1998): Cognitive
631 function in nondemented older women who took estrogen after menopause. *Neurology*.
632 50:368-373.
- 633 60. Yesufu A, Bandelow S, Hogervorst E (2007): Meta-analyses of the effect of hormone
634 treatment on cognitive function in postmenopausal women. *Women's Health*. 3:173-194.
- 635 61. Phillips SM, Sherwin BB (1992): Effects of estrogen on memory function in surgically
636 menopausal women. *Psychoneuroendocrinology*. 17:485-495.
- 637 62. Sherwin BB (1998): Estrogen and cognitive functioning in women. *Proc Soc Exp Biol*
638 *Med*. 217:17-22.
- 639 63. Sherwin BB (1997): Estrogen effects on cognition in menopausal women. *Neurology*.
640 48:215-265.
- 641 64. Luders E, Gaser C, Gingnell M, Engman J, Sundström Poromaa I, Kurth F (2021): Gray
642 matter increases within subregions of the hippocampal complex after pregnancy. *Brain*
643 *Imaging and Behavior*. 15:2790-2794.
- 644 65. Zeydan B, Tosakulwong N, Schwarz CG, Senjem ML, Gunter JL, Reid RI, et al. (2019):
645 Association of bilateral salpingo-oophorectomy before menopause onset with medial
646 temporal lobe neurodegeneration. *JAMA neurology*. 76:95-100.
- 647 66. Godsil BP, Kiss JP, Spedding M, Jay TM (2013): The hippocampal–prefrontal pathway:
648 the weak link in psychiatric disorders? *Eur Neuropsychopharmacol*. 23:1165-1181.
- 649 67. Bruce-Keller AJ, Keeling JL, Keller JN, Huang FF, Camondola S, Mattson MP (2000):
650 Antiinflammatory effects of estrogen on microglial activation. *Endocrinology*. 141:3646-3656.
- 651 68. Mazzucco C, Lieblich S, Bingham B, Williamson M, Viau V, Galea L (2006): Both estrogen
652 receptor α and estrogen receptor β agonists enhance cell proliferation in the dentate gyrus of
653 adult female rats. *Neuroscience*. 141:1793-1800.

- 654 69. Nagy AI, Ormerod BK, Mazzucco C, Galea LA (2005): Estradiol-induced enhancement in
655 cell proliferation is mediated through estrogen receptors in the dentate gyrus of adult female
656 rats. *Drug development research*. 66:142-149.
- 657 70. Waters EM, Mitterling K, Spencer JL, Mazid S, McEwen BS, Milner TA (2009): Estrogen
658 receptor alpha and beta specific agonists regulate expression of synaptic proteins in rat
659 hippocampus. *Brain Res*. 1290:1-11.
- 660 71. Brake WG, Alves SE, Dunlop JC, Lee SJ, Bulloch K, Allen PB, et al. (2001): Novel target
661 sites for estrogen action in the dorsal hippocampus: an examination of synaptic proteins.
662 *Endocrinology*. 142:1284-1289.
- 663 72. Wisse LE, Biessels GJ, Heringa SM, Kuijf HJ, Luijten PR, Geerlings MI, et al. (2014):
664 Hippocampal subfield volumes at 7T in early Alzheimer's disease and normal aging. *Neurobiol*
665 *Aging*. 35:2039-2045.
- 666 73. Deecher D, Andree TH, Sloan D, Schechter LE (2008): From menarche to menopause:
667 exploring the underlying biology of depression in women experiencing hormonal changes.
668 *Psychoneuroendocrinology*. 33:3-17.
- 669 74. Epperson CN, Steiner M, Hartlage SA, Eriksson E, Schmidt PJ, Jones I, et al. (2012):
670 Premenstrual dysphoric disorder: evidence for a new category for DSM-5. *Am J Psychiatry*.
671 169:465-475.
- 672 75. Rapkin AJ, Akopians AL (2012): Pathophysiology of premenstrual syndrome and
673 premenstrual dysphoric disorder. *Menopause international*. 18:52-59.
- 674 76. Gavin NI, Gaynes BN, Lohr KN, Meltzer-Brody S, Gartlehner G, Swinson T (2005):
675 Perinatal depression: a systematic review of prevalence and incidence. *Obstetrics &*
676 *Gynecology*. 106:1071-1083.
- 677 77. Freeman EW, Sammel MD, Boorman DW, Zhang R (2014): Longitudinal pattern of
678 depressive symptoms around natural menopause. *JAMA psychiatry*. 71:36-43.
- 679 78. ZORGDRAGER A, DE KEYSER J (1998): Premenstrual exacerbations of multiple sclerosis.
680 *Journal of Neurology, Neurosurgery & Psychiatry*. 65:279-280.
- 681 79. Confavreux C, Hutchinson M, Hours MM, Cortinovis-Tourniaire P, Moreau T, Group
682 PiMS (1998): Rate of pregnancy-related relapse in multiple sclerosis. *N Engl J Med*. 339:285-
683 291.
- 684 80. Ramagopalan SV, Dobson R, Meier UC, Giovannoni G (2010): Multiple sclerosis: risk
685 factors, prodromes, and potential causal pathways. *The Lancet Neurology*. 9:727-739.
- 686 81. Alvergne A, Tabor VH (2018): Is female health cyclical? Evolutionary perspectives on
687 menstruation. *Trends in ecology & evolution*. 33:399-414.
- 688 82. Travis S, Huang Y, Fujiwara E, Radomski A, Olsen F, Carter R, et al. (2014): High field
689 structural MRI reveals specific episodic memory correlates in the subfields of the
690 hippocampus. *Neuropsychologia*. 53:233-245.
- 691 83. Ogawa M, Sone D, Beheshti I, Maikusa N, Okita K, Takano H, et al. (2019): Association
692 between subfield volumes of the medial temporal lobe and cognitive assessments. *Heliyon*.
693 5:e01828.
- 694 84. Lee AC, Buckley MJ, Pegman SJ, Spiers H, Scahill VL, Gaffan D, et al. (2005):
695 Specialization in the medial temporal lobe for processing of objects and scenes. *Hippocampus*.
696 15:782-797.
- 697 85. Inhoff MC, Ranganath C (2015): Significance of objects in the perirhinal cortex. *Trends*
698 *in Cognitive Sciences*. 19:302-303.
- 699 86. Aminoff EM, Kveraga K, Bar M (2013): The role of the parahippocampal cortex in
700 cognition. *Trends in cognitive sciences*. 17:379-390.

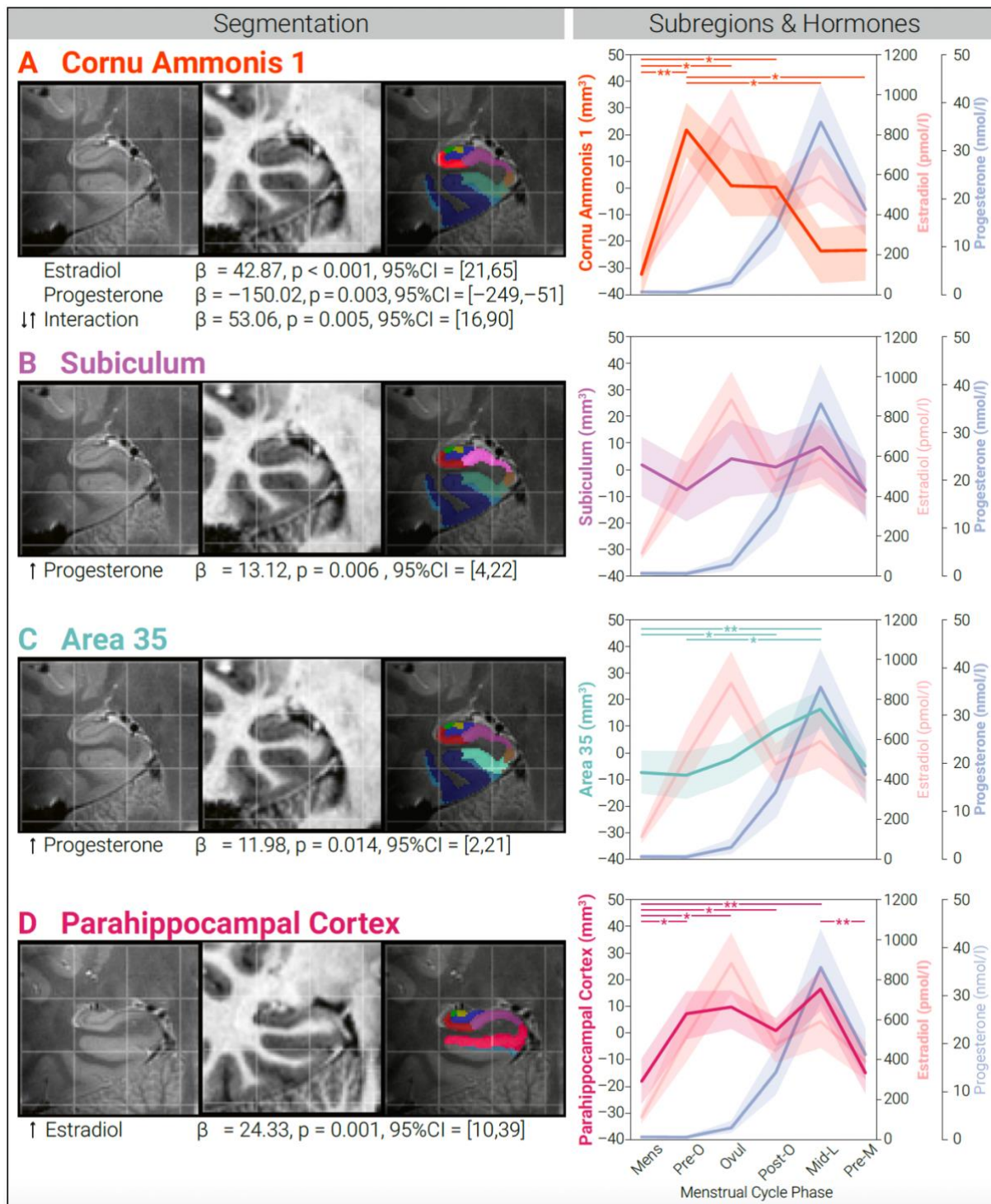
- 701 87. Jin J, Maren S (2015): Prefrontal-hippocampal interactions in memory and emotion.
702 *Frontiers in systems neuroscience*. 9:170.
- 703 88. Wang AC, Hara Y, Janssen WG, Rapp PR, Morrison JH (2010): Synaptic estrogen
704 receptor- α levels in prefrontal cortex in female rhesus monkeys and their correlation with
705 cognitive performance. *J Neurosci*. 30:12770-12776.
- 706 89. Beery AK, Zucker I (2011): Sex bias in neuroscience and biomedical research.
707 *Neuroscience & Biobehavioral Reviews*. 35:565-572.
- 708 90. Will TR, Proaño SB, Thomas AM, Kunz LM, Thompson KC, Ginnari LA, et al. (2017):
709 Problems and progress regarding sex bias and omission in neuroscience research. *eneuro*. 4.
- 710 91. Garcia-Sifuentes Y, Maney DL (2021): Reporting and misreporting of sex differences in
711 the biological sciences. *ELife*. 10:e70817.
- 712 92. Wittchen H-U, Wunderlich U, Gruschwitz S, Zaudig M (1997): SKID I. Strukturiertes
713 Klinisches Interview für DSM-IV. Achse I: Psychische Störungen. Interviewheft und
714 Beurteilungsheft. Eine deutschsprachige, erweiterte Bearb. d. amerikanischen Originalversion
715 des SKID I.
- 716 93. Fydrich T, Renneberg B, Schmitz B, Wittchen H-U (1997): SKID II. Strukturiertes
717 Klinisches Interview für DSM-IV, Achse II: Persönlichkeitsstörungen. Interviewheft. Eine
718 deutschsprachige, erw. Bearb. d. amerikanischen Originalversion d. SKID-II von: MB First, RL
719 Spitzer, M. Gibbon, JBW Williams, L. Benjamin,(Version 3/96).
- 720 94. Steiner M, Macdougall M, Brown E (2003): The premenstrual symptoms screening tool
721 (PSST) for clinicians. *Archives of Women's Mental Health*. 6:203-209.
- 722 95. O'Brien KR, Kober T, Hagmann P, Maeder P, Marques J, Lazeyras F, et al. (2014): Robust
723 T1-weighted structural brain imaging and morphometry at 7T using MP2RAGE. *PLoS ONE*.
724 9:e99676.
- 725 96. Luh WM, Wong EC, Bandettini PA, Hyde JS (1999): QUIPSS II with thin-slice T11 periodic
726 saturation: a method for improving accuracy of quantitative perfusion imaging using pulsed
727 arterial spin labeling. *Magnetic Resonance in Medicine: An Official Journal of the International*
728 *Society for Magnetic Resonance in Medicine*. 41:1246-1254.
- 729 97. Wong EC, Buxton RB, Frank LR (1998): A theoretical and experimental comparison of
730 continuous and pulsed arterial spin labeling techniques for quantitative perfusion imaging.
731 *Magn Reson Med*. 40:348-355.
- 732 98. RCore T (2013): R: A Language and Environment for Statistical Computing. R
733 Foundation for Statistical Computing [Internet]. Vienna, Austria.
- 734 99. Benjamini Y, Hochberg Y (1995): Controlling the false discovery rate: a practical and
735 powerful approach to multiple testing. *Journal of the Royal statistical society: series B*
736 *(Methodological)*. 57:289-300.
- 737
738

739 **Figures**
740



741
742
743
744
745
746
747
748
749

Figure 1: Changes in endogenous levels of estradiol, progesterone, luteinizing hormone (LH), and follicle-stimulating hormone (FSH) across menstrual cycle. Shaded area represents 95% confidence interval for hormone levels at menstrual (Mens), pre-ovulatory (Pre-O), ovulation (Ovul), post-ovulatory (Post-O), mid-luteal (Mid-L), and premenstrual (Pre-M) timepoints.



750
751
752
753
754
755
756
757
758
759
760
761

Figure 2: Changes in medial temporal lobe (MTL) volume associated with ovarian hormones across menstrual cycle. *Column 1:* Example T2-weighted image, T1-weighted image, and MTL segmentation for (A) cornu ammonis 1, (B) subiculum, (C) perirhinal Area 35, and (D) parahippocampal cortex. *Column 2:* After segmentation, unique associations between ovarian hormones and MTL regions across menstrual cycle. Linear mixed-effects model statistics reported in Column 2. Shaded area represents 95% confidence interval for hormone levels or subregion volumes. Asterisks refer to statistically significant changes in volume over timepoints, * $p < 0.05$, ** $p < 0.005$.

762 **Tables**

763

	Mean (mm³)	SD (mm³)	Range (mm³)
Total Brain Volume	1130246.38	83996.77	412000.00
Whole Hippocampus	5295.36	381.71	2322.00
CA1	1399.73	132.36	586.75
CA2	86.49	21.22	101.25
CA3	257.00	37.31	167.00
Dentate Gyrus	905.39	117.94	534.00
Subiculum	2043.41	146.34	739.25
Entorhinal Cortex	1151.98	165.34	852.50
Area 35	752.80	104.35	585.25
Area 36	4046.27	543.87	1959.25
Parahippocampal Cortex	660.92	97.75	540.00

764

765

766

767

Table 1 Descriptive statistics for each brain region volume, mm³. Whole hippocampus is the sum of cornu ammonis [CA] 1, CA2, CA3, subiculum, dentate gyrus, and remaining tail. Standard deviation [SD].